

# Top quark pair production cross section with the ATLAS experiment

Pedraza Lopez, S<sup>1,a</sup> on behalf the ATLAS Collaboration

<sup>1</sup>*Instituto de Fisica Corpuscular (IFIC)*

**Abstract.** This document reviews the existing results of inclusive top quark pair production cross section measurements in proton-proton collisions at a center of mass energies of 7 and 8 TeV performed with the ATLAS detector at the Large Hadron Collider. These measurements cover the different analysis channels, single lepton, dilepton and all hadronic channel, as well as dedicated analysis for channels including tau leptons decaying hadronically. All measurements shown in this document are in good agreement with the Standard Model expectation.

## 1 Introduction

The Large Hadron Collider (LHC) [1] has delivered a dataset of  $5 \text{ fb}^{-1}$  at  $\sqrt{s} = 7 \text{ TeV}$  in 2011 followed by a dataset of  $20 \text{ fb}^{-1}$  at  $\sqrt{s} = 8 \text{ TeV}$  in 2012. These two datasets have allowed the ATLAS experiment [2] to collect a large sample of top quark pairs ( $t\bar{t}$ ), providing the opportunity to perform precision measurements of the inclusive  $t\bar{t}$  cross section. These measurements are useful as a benchmark for QCD perturbative calculations, which are now available at full NNLO [3, 4]:

$$\sigma_{t\bar{t}}^{7\text{TeV}} = 172.0_{-5.8}^{+4.4}(\text{scale})_{-2.8}^{+4.7}(\text{pdf}) \text{ pb} \quad (1)$$

$$\sigma_{t\bar{t}}^{8\text{TeV}} = 245.8_{-8.4}^{+6.2}(\text{scale})_{-6.4}^{+6.2}(\text{pdf}) \text{ pb} \quad (2)$$

They are also expected to be sensitive to new physics in the top quark production and decay. While top quark pairs are produced through strong interaction (at LHC they are produced mainly via gluon fusion), the top quark decays through weak interaction into a  $W$  boson and a  $b$  quark with a branching ratio of almost 100%. Subsequently the  $W$  boson can decay either leptonically ( $W \rightarrow l\nu$ ) or hadronically ( $W \rightarrow q\bar{q}$ ). Therefore three different channels are defined to classify top quark pairs events: all hadronic (described in section 2), dileptonic (section 5) and single lepton or lepton plus jets (section 6). This document describes briefly seven recent measurements of the inclusive  $t\bar{t}$  production cross section ( $\sigma_{t\bar{t}}$ ) performed by the ATLAS experiment. All channels are covered using the 7 TeV sample, including two analysis for tau leptons decaying hadronically: tau plus lepton (section 4) and tau plus jets (section 3) channels. Finally, a measurement in the lepton plus jets channel is presented using the 8 TeV dataset.

---

<sup>a</sup>e-mail: sebastian.pedraza.lopez@cern.ch

## 2 All hadronic channel, $\sqrt{s} = 7 \text{ TeV}$

The all hadronic channel is the final state of  $t\bar{t}$  events with the largest branching ratio, however it suffers from a large QCD multi-jet background. The signal extraction is based on a kinematical fit that exploits the characteristic topology of an hadronic  $t\bar{t}$  event [5]: at least six jets, two of them identified as coming from the decay of a  $b$  quark, and no significant amount of missing transverse energy ( $E_T^{\text{miss}}$ ). The  $t\bar{t}$  event reconstruction is based on a maximization of a likelihood function to determine the best assignment of jets to the products of the top quark decay to obtain the top mass. Subsequently the top mass distributions built for signal, background and data are used in an unbinned likelihood fit to extract the  $\sigma_{t\bar{t}}$ , as it is shown in Figure 1. For the background modeling, the analysis technique derives the shape of the multi-jet background by performing the kinematical fit on the data sample without applying the  $b$ -tagging requirement. The effect of applying  $b$ -tagging on the top mass is checked with a separate sample. The measurement is based on a data sample corresponding to an integrated luminosity of  $4.7 \text{ fb}^{-1}$ . The dominant components of the total systematic uncertainty are jet energy scale uncertainty, with a relative uncertainty of 20%, and initial/final state radiation (ISR/FSR) and  $b$ -tagging efficiency, both with a relative uncertainty of 17%. The cross section measured has a value of:

$$\sigma_{t\bar{t}} = 168 \pm 12(\text{stat.})_{-57}^{+60}(\text{syst.}) \pm 7(\text{lumi.}) \text{ pb} \quad (3)$$

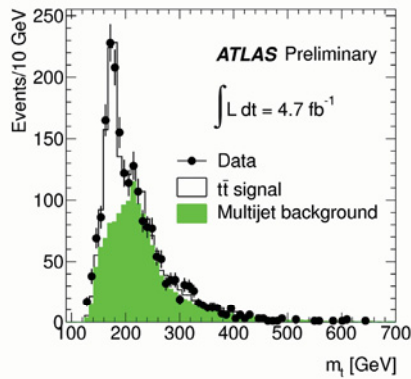


**Figure 1.** Fit of the top quark mass distribution with an unbinned likelihood to the selected data sample (dots). The signal and background templates are indicated as well [5].

## 3 Tau plus jets channel, $\sqrt{s} = 7 \text{ TeV}$

The tau plus jets channel consists of a final state with one  $W$  boson decaying to light quarks that hadronize to jets, while the other one decays to a tau neutrino and tau lepton which subsequently decays hadronically. The candidate events are selected with at least five jets, where two or more of them must be  $b$ -tagged jets. The main contributions to the background are other  $t\bar{t}$  channels, QCD multi-jets,  $W+$  jets and single-top production. A likelihood fit to the number of track distribution for the  $\tau$  candidate ( $n_{\text{track}}$ ) is performed with three templates [6]: the tau/electron template (containing signal event candidates), the gluon-jet template (mainly from QCD multi-jet events), and quark-jet template (from  $t\bar{t}$  background and  $W+$  jets), shown in Figure 2. The signal event candidates contain

both, real tau leptons and electrons which failed the electron veto. The tau/electron template is built using simulated  $t\bar{t}$  events and the relative contribution of taus and electrons is determined by Monte Carlo prediction. The gluon-jet template is built using data from a control region that enhances the contribution from gluon-initiated jets. The quark-jet template is also built using data, from a sample enriched in quark-initiated jets. The measurement is performed on a data sample corresponding to an integrated luminosity of  $1.67 \text{ fb}^{-1}$ . The dominant systematic uncertainties are ISR/FSR (15%), event generator model (11%) and  $b$ -tagging efficiency (9%). The cross section measured in this channel has a value of:

$$\sigma_{t\bar{t}} = 194 \pm 18(\text{stat.}) \pm 46(\text{syst.}) \text{ pb} \quad (4)$$

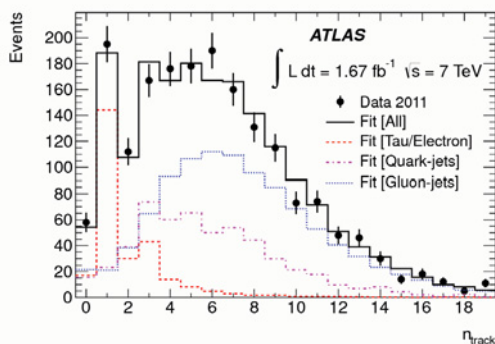


**Figure 2.**  $n_{\text{track}}$  distribution. The black points correspond to data, while the solid black line is the result of the fit. The red (dashed), blue (dotted) and magenta (dash-dotted) histograms show the fitted contributions from the  $\tau$  signal, and the gluon-jet and quark-jet backgrounds, respectively [6].

#### 4 Tau plus lepton channel, $\sqrt{s} = 7 \text{ TeV}$

In the tau plus lepton channel, one  $W$  boson decays to a tau lepton that decays hadronically while the other  $W$  decays into a electron or muon with the corresponding leptonic neutrino. The main background contributions in this channel are single lepton  $t\bar{t}$  events,  $W$  plus jets and QCD multi-jet. The events are selected with one electron or muon and three or more jets, with at least one of them  $b$ -tagged. Events are marked as same sign charge (SS) or opposite sign charge (OS) based on the reconstructed charge of the lepton and the tau candidate [7]. Since tau candidates in the SS sample are almost entirely fake tau leptons and candidates in the OS sample are a mixture of fake and real, as it is shown in Figure 3, the fake tau removal is achieved by subtracting SS events from the OS signal region. A boosted decision tree ( $\text{BDT}_j$ ) is employed to separate hadronic tau decays from jets in candidate events, yielding the distribution shown in Figure 3. The measurement is performed on a data sample corresponding to an integrated luminosity of  $2.05 \text{ fb}^{-1}$ . The cross section is extracted from a  $\chi^2$  fit of  $\text{BDT}_j$  OS-SS templates built for signal  $t\bar{t}$  events (with real taus and electrons failing the tau-electron veto) and a background template. This background template is obtained from a data sample with all the selection requirements expect  $b$ -tagging and requiring in addition zero  $b$ -jets. The expected amount of tau lepton signal is subtracted using MC and corrected bin by bin with the ratio of  $\geq 1$   $b$ -jet background to 0  $b$ -jet background:

$$\sigma_{t\bar{t}} = 186 \pm 13(\text{stat.}) \pm 20(\text{syst.}) \pm 7(\text{lumi.}) \text{ pb} \quad (5)$$

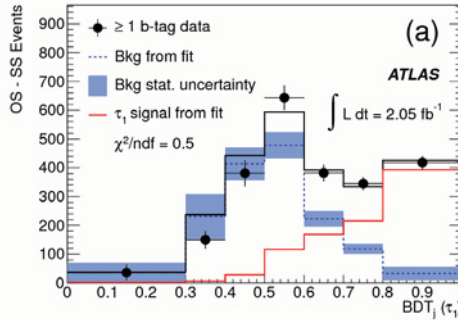


**Figure 3.**  $BDT_j$  (OS-SS) distributions of lepton plus single-track  $\tau$  candidates is shown. The normalisation of each template is derived from a fit to the data. The fitted contributions are shown as the light/red (signal), dashed/blue (background) and dark/black (total) lines. Shaded/blue bands are the statistical uncertainty of the background template [7].

The dominant systematic uncertainties for this analysis are  $b$ -jet tagging efficiency (9%), ISR/FSR modeling (4.8%) and the  $\tau$  identification (3%).

## 5 Dilepton channel, $\sqrt{s} = 7$ TeV

In the dilepton channel both  $W$  bosons decay to a lepton-neutrino pair in the final state. The event selection is based on the presence of two opposite sign leptons, two jets and large  $E_T^{\text{miss}}$ . Leptons are either well identified electron or muon candidates that are selected using the full detector or isolated tracks to reduce losses from lepton identification inefficiencies. The analysis is performed using eight channels that do not overlap between each other [8]:  $ee$ ,  $e\mu$ , and  $\mu\mu$  with and without requiring a  $b$ -tagged jet, and the two lepton plus track selection named  $eTL$  and  $\mu TL$ . The cross section is extracted from a profile likelihood for the individual channels and for the combination of channels, as it is shown in Figure 4, using the number of signal and background events after the event selection and the number of observed events in data. The measurement is based on a total integrated luminosity of  $0.70 \text{ fb}^{-1}$ . The main systematic uncertainties on the combined measurement are associated with the Monte Carlo generator (5%), the jet energy scale (4%) and lepton identification (3%). The cross section measured in this channel is found to be:

$$\sigma_{t\bar{t}} = 168 \pm 12(\text{stat.})_{-57}^{+60}(\text{syst.}) \pm 6(\text{lumi.}) \text{ pb} \quad (6)$$

## 6 Lepton plus jets channel

In the lepton plus jets channel, one of the two  $W$  bosons from the  $t\bar{t}$  pair decays into light quarks which subsequently hadronize into jets, while the other  $W$  boson decays to an electron, muon, or leptonically decaying tau lepton together with the corresponding neutrino. Three analysis have been performed in this channel, two at  $\sqrt{s} = 7$  TeV [9, 10] and the final one at  $\sqrt{s} = 8$  TeV [11]. The dominant background processes are  $W$ +jets and multi-jet production, which are estimated from data. A common event selection require one charge, isolated high  $p_T$  lepton and at least three jets, as well as a significant amount of missing transverse energy.

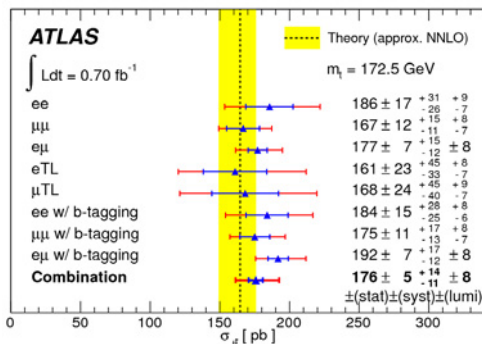


**Figure 4.** Summary of the individual cross section measurements and the combination result with and without  $b$ -tagging. The vertical dashed line and yellow band are the approximate NNLO theory calculation and its uncertainty [8].

### 6.1 $\sigma_{t\bar{t}}$ measured using kinematic information, $\sqrt{s} = 7$ TeV

This analysis utilizes a total integrated luminosity of  $0.70 \text{ fb}^{-1}$ . The dominant contributions to the background come from  $W$ +jets events and QCD multi-jet events, where one jet can be misidentified as a reconstructed lepton. Since the background from these sources is difficult to simulate correctly, its modeling is based on data. A likelihood discriminant is built using various kinematic variables ( $\eta(l)$ ,  $p_T(j)$ , Aplanarity<sup>1</sup>, and  $H_{T,3p}$ <sup>2</sup>). Templates are constructed for signal and backgrounds, splitting the sample in the electron and muon channel and different jet multiplicities. For this analysis no  $b$ -tagging is required. A profile likelihood fit including systematic uncertainties as nuisance parameters is performed in this distribution, as shown in Figure 5. The main systematic uncertainties are associated with the Monte Carlo generator (3%) and jet energy scale (2%). The cross section measured in this analysis is found to be:

$$\sigma_{t\bar{t}} = 179.0 \pm 3.9(\text{stat.}) \pm 9.0(\text{syst.}) \pm 6.6(\text{lumi.}) \text{ pb} \quad (7)$$

### 6.2 $\sigma_{t\bar{t}}$ measured using Soft Muon Tagging, $\sqrt{s} = 7$ TeV

This analysis exploits the full 7 TeV sample of  $4.66 \text{ fb}^{-1}$ . The Soft Muon Tagging (SMT) algorithm targets semimuonic B meson decays ( $b \rightarrow \mu X$ ) and makes use of a quality match between tracks in the inner detector and the muon spectrometer [10]. Selected events are required to have at least one SMT tagged jet, condition that enhances the amount of  $t\bar{t}$  signal events as it is shown in Figure 6. The main uncertainties in this analysis are the background modeling (7%), the jet energy scale (3.5%) and the experimental knowledge of the branching ratio of decays of b quarks generating muons (2.9%).

<sup>1</sup>Aplanarity,  $A$ , is defined as  $A = \frac{3}{2}\lambda_3$ , with  $\lambda_3$  being the smallest eigenvalue of the normalized momentum tensor calculated using the momenta of all jets and the lepton.

<sup>2</sup> $H_{T,3p}$  is the transverse momentum of all but the two leading jets, normalized to the sum of absolute values of all longitudinal momenta in the event.

The cross section is measured counting events passing the selection, and the value obtained is found to be:

$$\sigma_{t\bar{t}} = 165 \pm 2(\text{stat.}) \pm 17(\text{syst.}) \pm 3(\text{lumi.}) \text{ pb} \quad (8)$$

### 6.3 $\sigma_{t\bar{t}}$ measured using kinematic information, $\sqrt{s} = 8 \text{ TeV}$

The last analysis shown in this document is the only one available currently at  $\sqrt{s} = 8 \text{ TeV}$  sample, and it uses a total integrated luminosity of  $5.8 \text{ fb}^{-1}$ . In this case, the selection criteria is tightened to reduce the multi-jet background and at least one  $b$ -tagged jet is required. A likelihood discriminant is built with two kinematic variables,  $\eta(l)$  and the transformed Aplanarity  $A$ , shown in Figure 7. This discriminant exploits the kinematic differences between  $t\bar{t}$  signal events and  $W$  plus jets background events. The observed number of  $t\bar{t}$  events is extracted from a likelihood to binned distributions of this discriminant made for  $t\bar{t}$  signal, each of the backgrounds and the data. A negative log-likelihood fit is performed to obtain the  $t\bar{t}$  cross section, yielding a result of:

$$\sigma_{t\bar{t}} = 241 \pm 2(\text{stat.}) \pm 31(\text{syst.}) \pm 9(\text{lumi.}) \text{ pb} \quad (9)$$

The measurement is dominated by systematic uncertainty, being the main ones the signal modeling (11%) and jet related uncertainties (6%).

## 7 Summary

For the  $\sqrt{s} = 7 \text{ TeV}$  data sample all channels have been covered, allowing a good understanding of the detector and Monte Carlo generators. Three channels were combined using this dataset: lepton plus jets, dilepton and a previous analysis in the all hadronic channel, shown in Figure 8(a), yielding a combined result of [12]:

$$\sigma_{t\bar{t}} = 177 \pm 3(\text{stat.})_{-7}^{+8}(\text{syst.}) \pm 7(\text{lumi.}) \text{ pb} \quad (10)$$

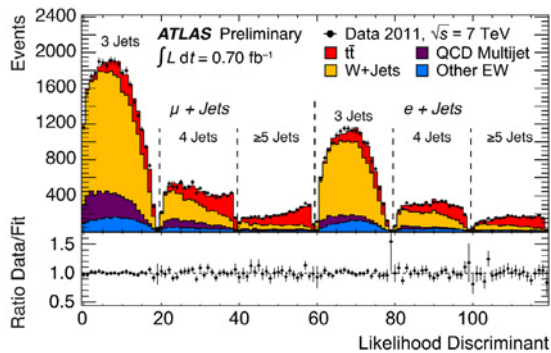


**Figure 5.** Result of combined fit to data of the electron+jets and  $\mu$ +jets channels. The lower plot shows the ratio of data to the sum of fitted signal and background contributions. Uncertainties on the ratio include data and MC statistical uncertainties [9].

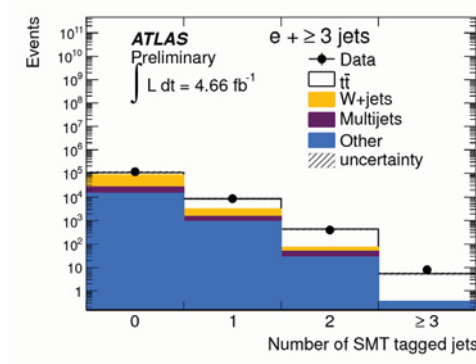


**Figure 6.** The figure shows the number of observed and expected jets per event in the  $e+\text{jets}$  tagged sample. "Other" denotes the smaller  $Z+\text{jets}$ , single top and diboson backgrounds which are estimated with Monte Carlo. Uncertainties include statistical and systematic contributions [10].

The analysis in the tau plus lepton and tau plus jets channels allow a test of flavor-dependent effects in top quark decays as well as studies for new physics searches, such as those predicting a charged Higgs boson decaying to a tau lepton plus a neutrino [13]. The results obtained in these dedicate channels as well as the rest results shown for the 7 TeV samples are in good agreement with the Standard Model predictions, as it is summarized in Figure 8(a).

The effort to analyse the large  $\sqrt{s} = 8$  TeV data sample is starting. The first result available was presented at section 6.3. The measurements at different center of mass energies, 7 and 8 TeV, are in good agreement with the evolution of the cross section with the center of mass energy predicted by the theory, as it is shown in Figure 8(b).

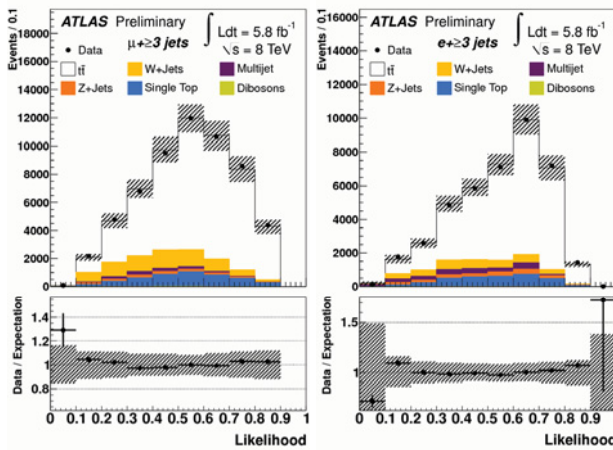
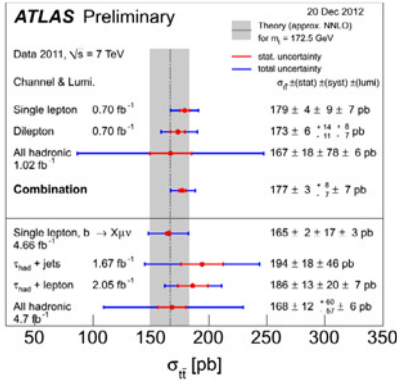
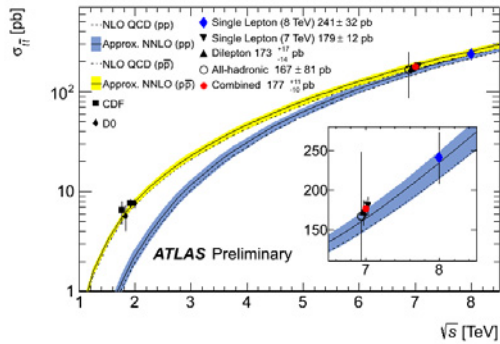


**Figure 7.** Fit to the likelihood discriminant distribution in the  $\mu+\text{jets}$  channel (left) and in the  $e+\text{jets}$  (right). The hatched bands display the combined expected statistical and systematic uncertainty [11].



(a) ATLAS combination of different channels using the  $\sqrt{s} = 7 \text{ TeV}$  dataset [12].



(b) Summary plot showing the top pair production cross section as a function of the LHC proton proton center of mass energy. The experimental results in the various top decay channels (and their combination) at 7 TeV and the recent result at 8 TeV are compared to an approximate NNLO QCD calculation based on Hather 1.2 [11, 12]

**Figure 8.** Summary plots for the  $\sigma_{tt}$  measurements available performed

## Acknowledgements

The work of the author is funded by the project FPA2012-39055-C02-01 of the Spanish Ministry of Economy and Competitiveness (MINECO). S.P.L. is under a contract belonging to the program VALi+D for research training of the Generalitat Valenciana.

## References

- [1] L. Evans and P. Bryant (editors), JINST **3**, S08001 (2008)
- [2] ATLAS Collaboration, JINST **3**, S08003 (2009)
- [3] M. Czakon, A. Mitov, JHEP **1301**, 080 (2013), arXiv:1210.6832 [hep-ph]
- [4] M. Czakon, P. Fiedler, A. Mitov, Phys.Rev.Lett. **110**, 252004(2013), arXiv:1303.6254 [hep-ph]
- [5] ATLAS Collaboration, ATLAS-CONF-2012-031 (2012)
- [6] ATLAS Collaboration, Eur.Phys.J. **C73**, 2328 (2013), arXiv:1211.7205 [hep-ex]
- [7] ATLAS Collaboration, Phys.Lett. **B717**, 89 (2012), arXiv:1205.2067 [hep-ex]
- [8] ATLAS Collaboration, JHEP **1205**, 059 (2012), arXiv:1202.4892 [hep-ex]
- [9] ATLAS Collaboration, ATLAS-CONF-2011-121 (2011)
- [10] ATLAS Collaboration, ATLAS-CONF-2012-131 (2012)
- [11] ATLAS Collaboration, ATLAS-CONF-2012-149 (2012)
- [12] ATLAS Collaboration, ATLAS-CONF-2012-024 (2012)
- [13] ATLAS Collaboration, ATLAS-CONF-2013-090 (2013)